

Reconstructing Patient-specific Cardiac Models from Contours via Delaunay Triangulation and Graph-cuts

Min Wan¹, Calvin Lim², Junmei Zhang¹, Yi Su², Si Yong Yeo², Desheng Wang³, Ru San Tan¹, Liang Zhong¹

Abstract—This study proposes a novel method to reconstruct the left cardiac structure from contours. Given the contours representing left ventricle (LV), left atrium (LA), and aorta (AO), re-orientation, contour matching, extrapolation, and interpolation are performed sequentially. The processed data are then reconstructed via a variational method. The weighted minimal surface model is revised to handle the multi-phase cases, which happens at the LV-LA-AO junction. A Delaunay-based tetrahedral mesh is generated to discretize the domain while the max-flow/min-cut algorithm is utilized as the minimization tool. The reconstructed model including LV, LA, and AO structure is extracted from the mesh and post-processed further. Numerical examples show the robustness and effectiveness of the proposed method.

I. INTRODUCTION

Cardiovascular Disease (CVD) is the leading cause of death nowadays, which killed 16.7 million people around the world each year, representing one third of total deaths. Reconstructing the patient-specific anatomic heart model is a prerequisite for quantitative analysis in normal and pathological conditions. The reliability of the evaluation of cardiac functions such as ventricle ejection fraction is also dependant on the precision and correctness of the heart modeling. The modeling problem could be further formulated as a surface reconstruction from a series of planar sectional contours, which are delineated manually or automatically.

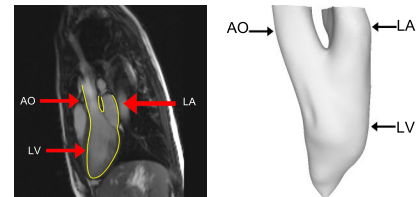
Medical imaging community also proposed a great number of approaches to establish the statistical heart model [1]–[7], which mainly use data to fit certain geometric shape combinations or statistic models. Researchers in numerical engineering also proposed various methods to reconstruct models from contours, which generally use triangulation and meshing technique to determine connections in between neighboring contours [8]–[11], which however suffer from the inevitable heuristics due to the topology variations or contours sparseness. The demand of a robust and precise reconstruction method motivates this study.

In our study, a novel method is proposed to reconstruct the patient-specific left cardiac model from contours via

¹M. Wan, et al. are with National Heart Centre Singapore, 17 Third Hospital Avenue, Mistri Wing, Singapore 168752. {wan.min, zhang.junmei, tan.ru.san, zhong.liang}@nhcs.com.sg

²C. Lim, et al. are with Institute of High Performance Computing, 1 Fusionopolis Way #16-16 Connexis, Singapore 138632. {limcw, suy1, yeosy}@ihpc.a-star.edu.sg

³D. Wang is with Division of Mathematical Sciences, School of Physical and Mathematical Sciences, Nanyang Technological University, Singapore 637371. desheng@ntu.edu.sg



(a) Vertical long axis view in cardiac MRI (b) Reconstructed left cardiac structure

Fig. 1. Illustration of left cardiac structure

Delaunay triangulation and graph-cuts. The input data are contours representing LV, LA, and AO. First, contours are re-orientated and matched to neighboring ones. The apex of LV is extrapolated and data are interpolated in between contours. The processed data are then input into a multi-phase variational surface reconstruction algorithm. A Delaunay based tetrahedral mesh is generated to discretize the domain of interest. The weighted minimal surface model [12] is adapted in our approach. The energy is discretized in the tetrahedral mesh and minimized via graph technique, i.e., max-flow/min-cut algorithm. The reconstructed surface model is further smoothed and remeshed for a better mesh quality.

The remainder of this paper is organized as follows. Section II presents the preprocessing tasks including contour re-orientation, matching, interpolation and extrapolation. In Section III, the variational reconstruction method is provided. Section IV gives a brief introduction of the surface smoothing and remeshing method. Section V gives the experimental results to demonstrate the effectiveness of the proposed method and Section VI concludes the article.

II. CONTOUR RE-ORIENTATION, MATCHING, INTERPOLATION, AND EXTRAPOLATION

The cardiac model reconstruction problem could be stated as: given a sequence of contour $\{V_i\}_{i=1}^K, \{A_i, O_i\}_{i=K+1}^L$, on the slice plane $Z_i, i = 1, 2, \dots, L$, find a surface S such that $S \cap Z_i$ would be an approximate of V_i or $A_i \cup O_i$. $V_i, A_i,$ and O_i represent the boundaries of LV, LA, and AO, respectively. Contours $V_i, A_i,$ and O_i are simple closed polygons without containment and intersections. See an example of left cardiac structure in Fig. 1 and contours in Fig. 2. The three groups of contours are combined into two contour sets, i.e., the LV-LA

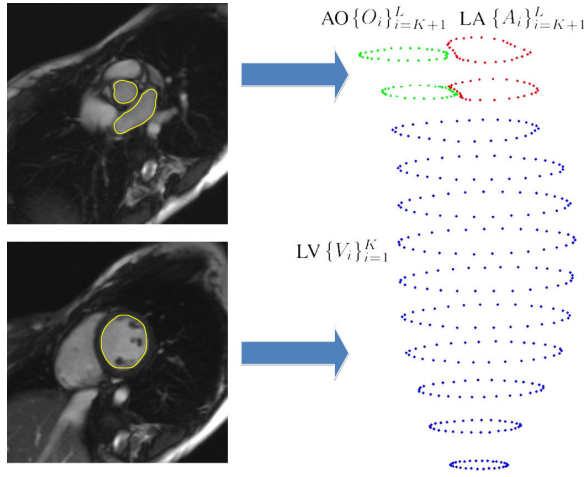


Fig. 2. Contours in 2D and 3D

set $\{ {}_1C_i \}_{i=1}^L$ and the LV-AO set $\{ {}_2C_i \}_{i=1}^L$ as follows.

$${}_1C_i = \begin{cases} V_i & i = 1, \dots, K \\ A_i & i = K + 1, \dots, L \end{cases} \quad (1)$$

$${}_2C_i = \begin{cases} V_i & i = 1, \dots, K \\ O_i & i = K + 1, \dots, L \end{cases} \quad (2)$$

All pre-processings are done on $\{ {}_1C_i \}_{i=1}^L$ and $\{ {}_2C_i \}_{i=1}^L$, respectively. From now on, $\{ C_i \}_{i=1}^L$ is used for short.

A. Contour Re-orientation and Matching

The first step in preprocessing is to establish consistency among all contours by performing contour re-orientation. All the polygons in $\{ C_i \}_{i=1}^L$ are re-oriented in the counter-clockwise direction. This task is accomplished via checking the signed area of the region bounded by the polygon or constructing the constrained Delaunay triangulation of the polygon.

Each contour C_i is then interpolated to a fixed number of vertices, such as N points. Contour matching between C_i and C_{i+1} is performed as the following steps.

- Find $\arg \min_{\delta} \sum_{j=0}^{N-1} d(C_{i,j} - C_{i+1,(j+\delta)_N})$;
- $C_{i+1,j} = C_{i+1,(j+\delta)_N}$,

where $C_{i,j}$ are vertices in the contour C_i and $(\cdot)_N$ is interpreted modulo N . These two steps are performed from $i = 1$ to $L - 1$, after which the correspondence between neighboring contours are established.

B. Contour Extrapolation and Interpolation

Due to the relatively large slice spacing in MR images, the apex of the LV usually does not appear in the contour data. Deriving a reasonable apex of the LV is important for reconstructing a complete and watertight LV model. Considering the fact that the LV has the approximate shape of a cone, we use the centroids of each LV contour to compute an apex via cubic spline extrapolating scheme.

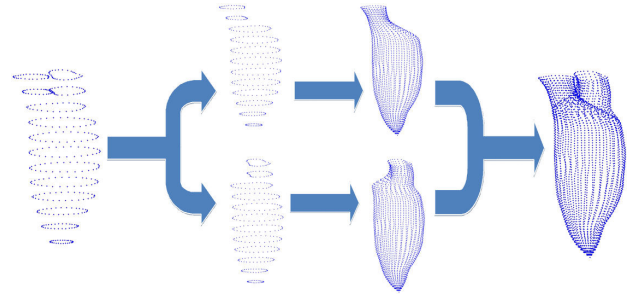


Fig. 3. Flowchart of preprocessing

- Compute centroid M_i for each V_i on plane Z_i ;
- Extrapolate the apex position M_0 using $\{ M_i \}_{i=1}^K$.

The apex has a one-to- N correspondence to the other contours. We extend the Z level from $1, \dots, K$ to $0, \dots, K$. $V_{0,j} = M_0$ for $j = 0, \dots, N - 1$. This new contour V_0 is also added into $\{ C_i \}$.

For each group of corresponding data points $\{ C_{i,j} \}_{i=0}^L$, interpolation is conducted. Interpolating scheme is cubic spline and interpolation parameter is estimated based on slice spacing and pixel spacing. Two interpolated data sets are obtained at the end of the preprocessing stage. Fig. 3 gives a flowchart for this section.

III. MULTI-PHASE SURFACE RECONSTRUCTION BASED ON DELAUNAY TRIANGULATION AND GRAPH-CUTS

Two point sets have been obtained from interpolation and extrapolation of contour points in Section 2. We adapt the model by adding an area regularization term.

$$E(S) = \sum_{S=\cup_i S_i} \int_{S_i} (d(x, P) + \alpha) ds, \quad (3)$$

where S_i is each patch of surface, i.e., the interface of each pair of different partitions; α is the regularization coefficient, which controls the smoothness of reconstructed model.

A. Delaunay based Mesh Framework

We denote the union of two point sets by P . As suggested in [13], the Delaunay triangulation is generated as the background mesh for the subsequent energy minimization procedure, see a 2D illustration in Fig. 4(a).

The surface reconstruction problem is then equivalent to a labelling problem for all tetrahedra elements K_i in the mesh. On the tetrahedral mesh, the surface is discretized to a triangulated mesh, which is the union of all triangles shared by two tetrahedra with different labels.

The discrete energy in mesh \mathcal{T} is

$$\begin{aligned} E(S) &= \int_S (d(x, P) + \alpha) ds \\ &= \sum_{i \neq j} \int_{K_i \cap K_j} (d(x, P) + \alpha) ds \\ &= \sum_{i \neq j} (d_{i,j} + \alpha) s_{i,j} \mathbf{1}_{\{l_i \neq l_j\}}. \end{aligned} \quad (4)$$

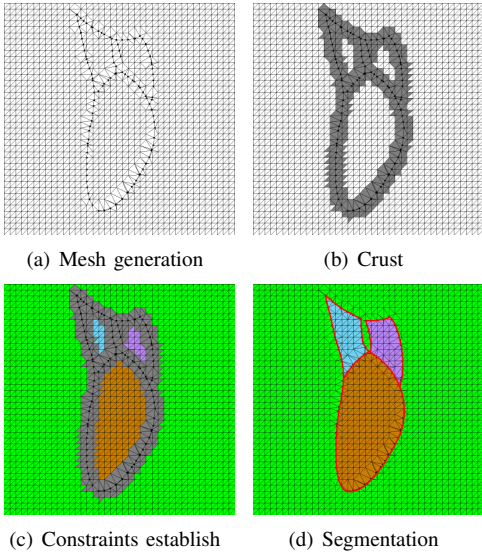


Fig. 4. 2D illustration of reconstruction

B. Establishment of Constraints

Minimizing the unconstrained energy in (4) will obtain a trivial solution: all elements in \mathcal{T} are labeled identically and the surface is null, obviously a useless solution. Hence, to obtain a non-trivial solution, some predefined constraints must be set for the energy functional in (4).

In our study, the constraint placed on the model is derived from the fact that at least two elements shall be labeled differently. Certain labels shall be assigned prior to some elements which are known to be interior or exterior. In order to pick up these elements with prior labelling, the ‘‘crust’’ around P is used to separate the domain. The crust is defined as $C_P^M = \{K_i \exists v \in K_i, v \in N_u^M, u \in P\}$, where N_u^M is the M -ring neighborhood of vertex u . In our study, C_P^1 is chosen to be the crust (Fig. 4(b)). After establishing the crust, the prior labelling work could be conducted by a region growing method [14] and the C_P^1 serves as the watershed in the algorithm.

After establishing constraints, the energy in (4) is modified to:

$$E_A(S) = \sum_{i \neq j} (d_{i,j} + \alpha) s_{i,j} \mathbf{1}_{\{I_i \neq I_j\}} + C \sum_{i=1}^{N_K} |I_i - I_i| \mathbf{1}_{\{I_i \neq 0\}}, \quad (5)$$

where I_i serves as the prior labelling. Fig. 4(c) illustrates different I_i using different colors.

C. Minimization via graph-cuts

Based on our previous study in [13], the energy in (5) is graph-representable. Then a graph dual to the tetrahedral mesh is generated as shown in Fig. 5(a) and (b). The edge weights (Fig. 5(c)) are determined by the energy functional in [5] and assigned in [6].

$$\begin{aligned} s_i &= C |I_i - 2| \mathbf{1}_{\{I_i \neq 0\}}, & s_j &= C |I_j - 2| \mathbf{1}_{\{I_j \neq 0\}}, \\ t_i &= C |I_i - 1| \mathbf{1}_{\{I_i \neq 0\}}, & t_j &= C |I_j - 1| \mathbf{1}_{\{I_j \neq 0\}}, \\ n_{ij} &= (d_{ij} + \alpha) s_{ij}, & n_{ji} &= (d_{ij} + \alpha) s_{ij}. \end{aligned} \quad (6)$$

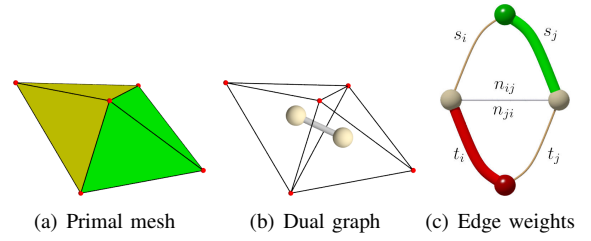


Fig. 5. Graph construction

The energy minimization task is accomplished by an efficient combinatorial optimization tool, i.e., max-flow/min-cut algorithm [15]. Fig. 4(d) illustrates the multi-phase segmentation result. After the minimal cut of the dual graph is obtained, the surface is then extracted from the tetrahedral mesh according to the cut. The interior artificial surfaces in the model are detected and removed.

IV. SURFACE SMOOTHING AND REMESHING

After obtaining the reconstruction result, certain post-processing is required to achieve a triangulated mesh model of appropriate quality for downstream numerical simulation. In this section, we describe two post-processing methods used in our study, i.e., smoothing and remeshing.

An improved Laplacian smoothing algorithm [16] is adopted in our method. Compared with classical Laplacian smoothing which pulls each vertex towards the average of its neighborhood, this variation has one extra operation: it pushes each vertex to a weighted combination of its original position and its previous position. This extra step helps to eliminate volume shrinkage evident in classical Laplacian smoothing.

The remeshing algorithm in [17] is used in our study. First, normalized edge lengths are computed based on geometric metric and mesh sizing function [18]. Edge splitting and contraction are conducted using the criterion of $\sqrt{2}$ and $\frac{1}{\sqrt{2}}$, respectively. Meanwhile, edge flipping is also done in each iteration to improve the triangle mesh quality.

V. NUMERICAL EXPERIMENTS

The proposed method was experimented on 17 subjects (thirteen males and six females; mean age 39, range from 19 to 70). The cine MR images were acquired on a 1.5T Siemens scanner with ECG gating. The slice thickness is 8 mm. The pixel spacing is typically 1.46 mm. The TR/TE/flip angle is typically $68ms/1ms/70^\circ$. A cine image contains around 20 to 22 time frames over a cardiac cycle.

One example of a reconstructed model is shown from its long-axis cross sectional view and zoomed view of the LV-LA-AO junction in Fig. 6. Six models out of 22 frames are shown in Fig. 7 starting from the end diastole (ED) phase.

From the experiment, we could observe a smooth and anatomically reasonable left cardiac structure, especially the LV-LA-AO junction region. The visual resemblance between the long-axis cross section view of reconstruction in Fig. 6(c) and the long-axis MR image also validate our method.

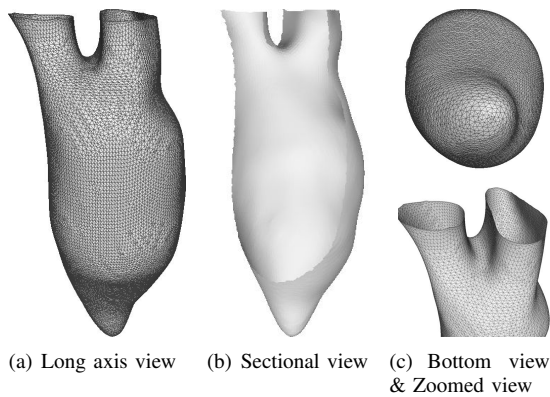


Fig. 6. Reconstructed result

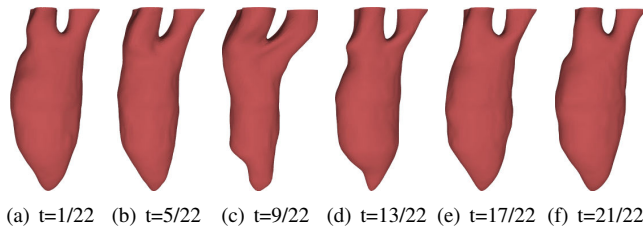


Fig. 7. Six selected frames from one cardiac cycle

Statistics of surface mesh quality of the example are shown in Fig. 8. The criterion for (a) is based on [19] and (b) is the triangle angle distribution.

VI. CONCLUSION

In this article, a novel automatic model reconstruction method for the left cardiac structure is proposed based on Delaunay triangulation and graph-cuts. Given the acquired MR images and contours representing LV, LA, and AO, preprocessing is performed using contour re-orientation, contour matching, interpolation, extrapolation. The processed data is then reconstructed via the minimization procedure of a variational surface model. A Delaunay based tetrahedral mesh is used for discretization and graph techniques are applied to minimize the energy functional. The surface model corresponding to the minimizer is then extracted and post-processed, such as smoothing and remeshing. Our experiments show the effectiveness of the proposed method.

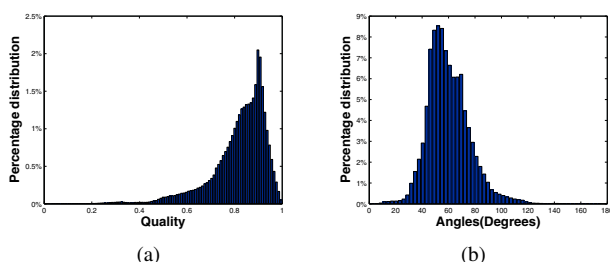


Fig. 8. Quality Statistics

ACKNOWLEDGMENT

This work was supported in part by research grants from the National Medical Research Council (NMRC/EDG/1037/2011), the National Research Foundation (NRF2011NRF- POC001-068), and SingHealth Foundation Research Grant (SHF/FG503P/2012).

REFERENCES

- [1] D. McQueen and C. Peskin, "A three-dimensional computer model of the human heart for studying cardiac fluid dynamics," *ACM SIG-GRAPH Computer Graphics*, vol. 34, no. 1, pp. 56–60, 2000.
- [2] L. Zhukov, Z. Bao, I. Guskov, J. Wood, and D. Breen, "Dynamic deformable models for 3d mri heart segmentation," in *SPIE Medical Imaging*, vol. 4684, 2002, pp. 1398–1405.
- [3] M. Sermesant, C. Forest, X. Pennec, H. Delingette, and N. Ayache, "Deformable biomechanical models: Application to 4d cardiac image analysis," *Medical Image Analysis*, vol. 7, no. 4, pp. 475–488, 2003.
- [4] J. Von Berg and C. Lorenz, "Multi-surface cardiac modelling, segmentation, and tracking," *Functional Imaging and Modeling of the Heart*, pp. 808–808, 2005.
- [5] C. Lorenz and J. von Berg, "Towards a comprehensive geometric model of the heart," *Functional Imaging and Modeling of the Heart*, pp. 102–112, 2005.
- [6] C. Lorenz and J. Berg, "A comprehensive shape model of the heart," *Medical image analysis*, vol. 10, no. 4, pp. 657–670, 2006.
- [7] Y. Zheng, A. Barbu, B. Georgescu, M. Scheuering, and D. Comaniciu, "Four-chamber heart modeling and automatic segmentation for 3-d cardiac ct volumes using marginal space learning and steerable features," *Medical Imaging, IEEE Transactions on*, vol. 27, no. 11, pp. 1668–1681, 2008.
- [8] C. Bajaj, E. Coyle, and K. Lin, "Arbitrary topology shape reconstruction from planar cross sections," 1995.
- [9] J. Boissonnat, "Shape reconstruction from planar cross sections," *Computer Vision, Graphics, and Image Processing*, vol. 44, no. 1, pp. 1–29, 1988.
- [10] J. Oliva, M. Perrin, and S. Coquillart, "3d reconstruction of complex polyhedral shapes from contours using a simplified generalized voronoi diagram," in *Computer Graphics Forum*, vol. 15, no. 3. Wiley Online Library, 1996, pp. 397–408.
- [11] S. Bereg, M. Jiang, and B. Zhu, "Contour interpolation with bounded dihedral angles," in *Proceedings of the ninth ACM symposium on Solid modeling and applications*. Eurographics Association, 2004, pp. 303–308.
- [12] H. Zhao, S. Osher, and R. Fedkiw, "Fast surface reconstruction using the level set method," in *Variational and Level Set Methods in Computer Vision, 2001. Proceedings. IEEE Workshop on*. IEEE, 2001, pp. 194–201.
- [13] M. Wan, Y. Wang, and D. Wang, "Variational surface reconstruction based on delaunay triangulation and graph cut," *International journal for numerical methods in engineering*, vol. 85, no. 2, pp. 206–229, 2011.
- [14] R. Adams and L. Bischof, "Seeded region growing," *Pattern Analysis and Machine Intelligence, IEEE Transactions on*, vol. 16, no. 6, pp. 641–647, 1994.
- [15] Y. Boykov and V. Kolmogorov, "An experimental comparison of min-cut/max-flow algorithms for energy minimization in vision," *Pattern Analysis and Machine Intelligence, IEEE Transactions on*, vol. 26, no. 9, pp. 1124–1137, 2004.
- [16] J. Vollmer, R. Mencl, and H. Mueller, "Improved laplacian smoothing of noisy surface meshes," in *Computer Graphics Forum*, vol. 18, no. 3. Wiley Online Library, 1999, pp. 131–138.
- [17] D. Wang, O. Hassan, K. Morgan, and N. Weatherill, "Enhanced remeshing from stl files with applications to surface grid generation," *Communications in numerical methods in engineering*, vol. 23, no. 3, pp. 227–239, 2007.
- [18] P. Frey *et al.*, "About surface remeshing," 2000.
- [19] P. Frey and H. Borouchaki, "Surface mesh quality evaluation," *International journal for numerical methods in engineering*, vol. 45, no. 1, pp. 101–118, 1999.